Carcinogenesis, 2017, Vol. 38, No. 8, 797–805

doi:10.1093/carcin/bgx057
Advance Access publication June 16, 2017
Original Article

ORIGINAL ARTICLE

DNA methylation signatures and coagulation factors in the peripheral blood leucocytes of epithelial ovarian cancer

Lian Li, Hong Zheng, Yubei Huang, Caiyun Huang, Shuang Zhang, Jing Tian[1], Pei Li, Anil K.Sood[2], Wei Zhang[3] and Kexin Chen*

Department of Epidemiology and Biostatistics, [1]Department of Urology, National Clinical Research Center for Cancer, Key Laboratory of Cancer Prevention and Therapy of Tianjin, Tianjin Medical University Cancer Institute and Hospital, Tianjin 300060, China, [2]Gynecologic Oncology and Reproductive Medicine and Center for RNAi and Non-Coding RNA, The University of Texas MD Anderson Cancer Center, Houston, TX 77030, USA and [3]Department of Cancer Biology, Wake Forest Baptist Comprehensive Cancer Center, Winston-Salem, NC 27157, USA

*To whom correspondence should be addressed. Tel: +86 (0)2223372231; Fax: +86 (0)2223372231; Email: chenkexin@tjmuch.com
Correspondence may also be addressed to Wei Zhang. Tel: +1 336 713 7508; Fax: +1 336 713 7566; Email: wezhang@wakehealth.edu

Abstract

Solid tumors are increasingly recognized as a systemic disease that is manifested by changes in DNA, RNA, proteins and metabolites in the blood. Whereas many studies have reported gene mutation events in the circulation, few studies have focused on epigenetic DNA methylation markers. To identify DNA methylation biomarkers in peripheral blood for ovarian cancer, we performed a two-stage epigenome-wide association study. In the discovery stage, we measured genome wide DNA methylation for 485 000 CpG sites in peripheral blood in 24 epithelial ovarian cancer (EOC) cases and 24 age-matched healthy controls. We selected 96 significantly differentially methylated CpG sites for validation using Illumina's Custom VeraCode methylation assay in 206 EOC cases and 205 controls and 46 CpG sites validated in the independent replication samples. A set of 6 of these 46 CpG sites was found by the receiver operating characteristic analysis to have a prediction accuracy of 77.3% for all EOC (95% confidence interval: 72.9–81.8%). Pathway analysis of the genes associated with the 46 CpG sites revealed an enrichment of immune system process genes, including *LYST* (cg16962115, *FDR* = 1.24E–04), *CADM1* (cg21933078, *FDR* = 1.22E–02) and *NFATC1* (cg06784563, *FDR* = 1.46E–02). Furthermore, DNA methylation status in peripheral blood was correlated with platelet parameters/coagulation factor levels. This study discovered a panel of epigenetic liquid biopsy markers closely associated with overall immunologic conditions and platelet parameters/coagulation systems of the patients for detection of all stages and subtypes of EOC.

Introduction

Ovarian cancer is the most lethal gynecologic cancer world wide (1). The two main reasons for the high death rate are lack of early detection and chemoresistance (2). Although ovarian cancer patients respond to initial chemotherapy, approximately 25% of patients develop chemotherapeutic drug resistance within 6 months (3). Extensive investigations in the tumor tissues have revealed heterogeneous genetic and epigenetic alterations underlying ovarian cancer development and progression. Developing effective early detection biomarkers, especially in the circulation, is critically needed for improving the outcome of women with ovarian cancer.

It is well established that tumor cells lyse and release DNA fragment (cfDNA or cell free DNA) as well as other molecules such as miRNA and cytokines to circulation (4). These tumor associated cfDNAs in the circulation are the basis for mutation detection in genes known to be altered in cancer especially in

Received: March 24, 2017; **Revised:** May 30, 2017; **Accepted:** June 5, 2017

Abbreviations

EOC	epithelial ovarian cancer
FDR	false discovery rate

the advanced stages when mutant DNAs are relatively abundant in the blood for detection. Mutation detection for early stage cancer is challenging due to the limited release of tumor cfDNA in the circulation when tumors are restricted locally. In addition, early tumor driving events may be epigenetic in nature, and defy mutation-based detection.

The recent successes in check-point immunotherapy have revived the recognition that cancer is a systemic disease that can be directly affected by the immune system (5). Emerging evidence has revealed that specific types of immune cells play a profound role in ovarian cancer cell proliferation and metastasis (6–8). Therefore, immune cells may represent a window to explore cancer pathogenesis and physiological homeostasis. Events associated with the immune system may be ideal biomarkers for cancer, especially in early stages. It is conceivable that genetic or epigenetic alterations in tumor cells would trigger immune surveillance and immune cells would undergo epigenetic reprogramming in order to counteract the appearance of cancer cells.

Recently, peripheral blood-derived DNA methylation profiles have been found to be associated with several cancer types such as breast, lung, gastric, ovarian and pancreatic cancer (9–15). Previous epigenome wide association studies of blood-based DNA methylation biomarkers for ovarian cancer risk were performed with a low density platform with coverage of 27 000 CpGs (12,16–18). Thus, we undertook the present study to explore the potential value of leukocyte DNA methylation in epithelial ovarian cancer (EOC). We conducted a two-stage case–control study basing on the epigenome-wide association study in Chinese EOC patients. In the discovery stage, 450 000 CpGs were scanned in genome-wide methylation array, and differentially methylated CpG sites were selected for validating in validation stage.

Materials and Methods

Study population

Ovarian cancer cases were women aged 25–85 years with histologically confirmed primary EOC between 2007 and 2013 in Tianjin Medical University Cancer Hospital. Patients with a previous medical history of cancer or blood transfusion within preceding 6 months were excluded. Patient blood samples were collected in the operating room and the values of blood cell counts and coagulation factors were obtained from the routine blood test and routine coagulation test that was conducted within a week before operation. Controls were cancer-free subjects from communities in Tianjin, who had no previous diagnosis of cancer and frequency-matched (with 5-year interval) to cases on age. Each subject completed questionnaires (including demographic information, health conditions, lifestyle and dietary habits) and provided blood samples for research. This study was approved by the Institutional Review Board of Tianjin Medical University Cancer Institute and Hospital, and informed consent was obtained for use of clinical specimens for research.

In the discovery stage, 24 EOC cases (12 cases with FIGO stages I–II and 12 cases with FIGO stages III–IV) and age-frequency matched controls were randomly selected for genome-wide methylation profiling. In validation stage, 206 EOC cases and 205 age-frequency matched controls were included in validation of the CpG sites selected in phase I.

DNA extraction and bisulfate conversion

Genomic DNA from sample collections was extracted from leukocytes by Qiazen DNA Blood Mini Kit (Qiazen, Valencia, CA), and stored at –80°C until bisulfite modification. By treating the genomic DNA using the bisulfate conversion kit of EZ-96 DNA Methylation-Gold Kit (D5008) (Zymo Research, Orange, CA) according to the manufacturer's protocol, the unmethylated cytosine was converted into uracil and the methylated cytosine remained unchanged. Bisulfite converted DNA was stored at –20°C, and used within one week after conversion.

Genome-wide methylation profiling

In the discovery stage, the genome-wide methylation profiling was conducted utilizing Illumina Infinium HumanMethylation450 BeadChip (San Diego, CA). We imaged the arrays with the Illumina BeadArray™ Reader and obtained the data using Illumina's GenomeStudio software. All samples passed quality control test, which included staining controls, extension controls, target removal controls, hybridization controls, bisulfate conversion controls, specificity controls, negative controls and non-polymorphic binding controls. Background normalization was performed with negative control bead in each well. DNA methylation value (β-value) of each CpG site was ranged from 0 (unmethylated) to 1 (methylated), represented by the relative ratio of methylated allele signals to total fluorescent signals after subtracting background intensity.

Validation of selected CpG loci

In validation stage, the Illunima's Custom VeraCode methylation assay (96-plex) was designed for validation studies of 96 selected CpG loci. Illunima's BeadXpress Reader scanner and Illumina's GenomeStudio were used to scan the beadchip and obtain data, respectively. A quality control test was completed including nine internal controls (allele-specific extension controls, PCR uniformity controls, extension gap controls, gender controls, first hybridization controls, second hybridization controls, negative controls and contamination detection controls). One CpG site (cg26366833) failed to genotype in validation; therefore, 95 CpG sites passed quality control, and the calculation of methylation value was the same to the HumanMethylation450 BeadChips. Thirteen samples were examined twice for technical replication, high correlation was observed between the replication samples ($r^2 > 0.98$).

Gene expression analysis

The gene expression microarray data is publicly available from Gene Expression Omibus (GEO, http://www.ncbi.nlm.nih.gov/geo/, Accession number GSE31682), and consisted of 48 ovarian cancer cases and controls (19). The difference of gene expression of the three genes in blood cells between cases and controls was carried out using independent *t*-test.

Statistical analysis

To compare the demographic characteristics between cases and controls, χ^2 test and independent *t*-test were used for categorical variables and continuous values, respectively. In the initial discovery stage, the difference of median β-value between cases and controls for each CpG site was carried out using independent *t*-test. Stratified analysis according to stage of EOC (I–II, III–IV) was also performed. We then selected 96 top differentially methylated CpG sites from the genome-wide scan for validation as following: (a) $P < 1.0 \times 10^{-4}$; (b) the same direction between I–II EOC cases and III–IV EOC cases when compared with controls; and (c) available for epigenotyping using Illunima's Custom VeraCode methylation assay. In the validation stage, an independent *t*-test was used to assess the difference of methylation values between study groups. The Pearson correlation analysis was conducted to evaluate the correlation between DNA methylation and blood cell counts/coagulation factors. To correct for multiple testing, Benjamini and Hochberg correction method was utilized to calculate the false discovery rate (FDR), and FDR < 0.05 was considered to be significant.

Furthermore, to evaluate the classifier performance of differentially methylated CpG sites in validation stage, we utilized a logistic regression model to build the predicting model of receiver operating characteristic curves. DNA methylation markers were selected using stepwise and manual selection method.

Additionally, to identify the commonality of genes within biological pathways, we utilized the DAVID gene ontology tool for the pathway enrichment analysis, which was conducted for the genes near the differentially methylated CpG sites associated with ovarian cancer risk. All

analyses were carried out using SAS version 9.3 (SAS Institute, Cary, NC) and R version 3.1.2.

Results

To identify differential DNA methylation in peripheral blood leukocytes in ovarian cancer, we conducted two stage case–control epigenome-wide association study (EWAS). A flowchart of the study design was shown in Figure 1. For the initial discovery stage, genome-wide scan were performed using Illumina's Infinium Humanmethylation450K beadchip in 24 EOC cases and 24 age-matched health controls. There was no significant difference in age, BMI, smoking status, family history of cancer and menopausal status between cases and controls. All of the cases were serous ovarian cancer; 12 were early stage and 12 were late stage (Supplementary Table 1, available at *Carcinogenesis* Online). Manhattan plot showed the epigenome wide analysis result (Figure 2). The methylation levels of 242 CpG sites exhibited significant differences between the 24 EOC cases and 24 controls ($P < 1.0 \times 10^{-4}$). When stratified by stage, 39 CpG sites were significantly different in 12 early stage (stages I and II) EOC cases, and 375 CpG loci in 12 advanced stage (stages III and IV) EOC cases when compared to 24 controls ($P < 1.0 \times 10^{-4}$). Volcano plots of differentially methylated CpG sites are shown in Supplementary Figure 2, available at *Carcinogenesis* Online. We selected 96 significant CpG sites for validation in the next stage (Supplementary Table 2, available at *Carcinogenesis* Online).

We evaluated the selected 96 CpG methylation sites in an independent set of 206 EOC cases and 205 controls using Illunima's Custom VeraCode methylation assay. Cases and controls were similar with regard to age, BMI, smoking status, Family history of cancer and menopausal status (Supplementary Table 1, available at *Carcinogenesis* Online). We found that 40 CpG sites were significantly associated with risk of EOC (FDR < 0.05), which were 16 hyperM (hypermethylated) and 24 hypoM (hypomethylated) (Figure 3; Supplementary Table 3, available at *Carcinogenesis* Online). In stratified analysis of stage, DNA methylations of 24 CpG sites (9 hypoM and 15 hyperM) were significantly different between 88 early stage (stages I and II) cases and controls, 39 CpG sites (21 hypoM and 18 hyperM) were significantly different between 115 advanced stage (stages III and IV) cases and controls. We also evaluated the methylation difference between cases and controls after stratifying cases by histological subtype. We identified 32 sites that were significantly differentially methylated in 85 Serous ovarian cancer, 34 CpG sites in 59 Endometrioid ovarian cancer, and 11 CpG sites in 24 Mucinous ovarian cancers when compared to 205 controls (Figure 3; Supplementary Table 4, available at *Carcinogenesis* Online). In total, we identified 46 CpG sites that were significantly differentially methylated in any of comparisons.

Receiver operating characteristic curves of single CpG site were presented in Supplementary Figures 3–8, available at *Carcinogenesis* Online. Six GpG sites (cg00207226, cg01535567,

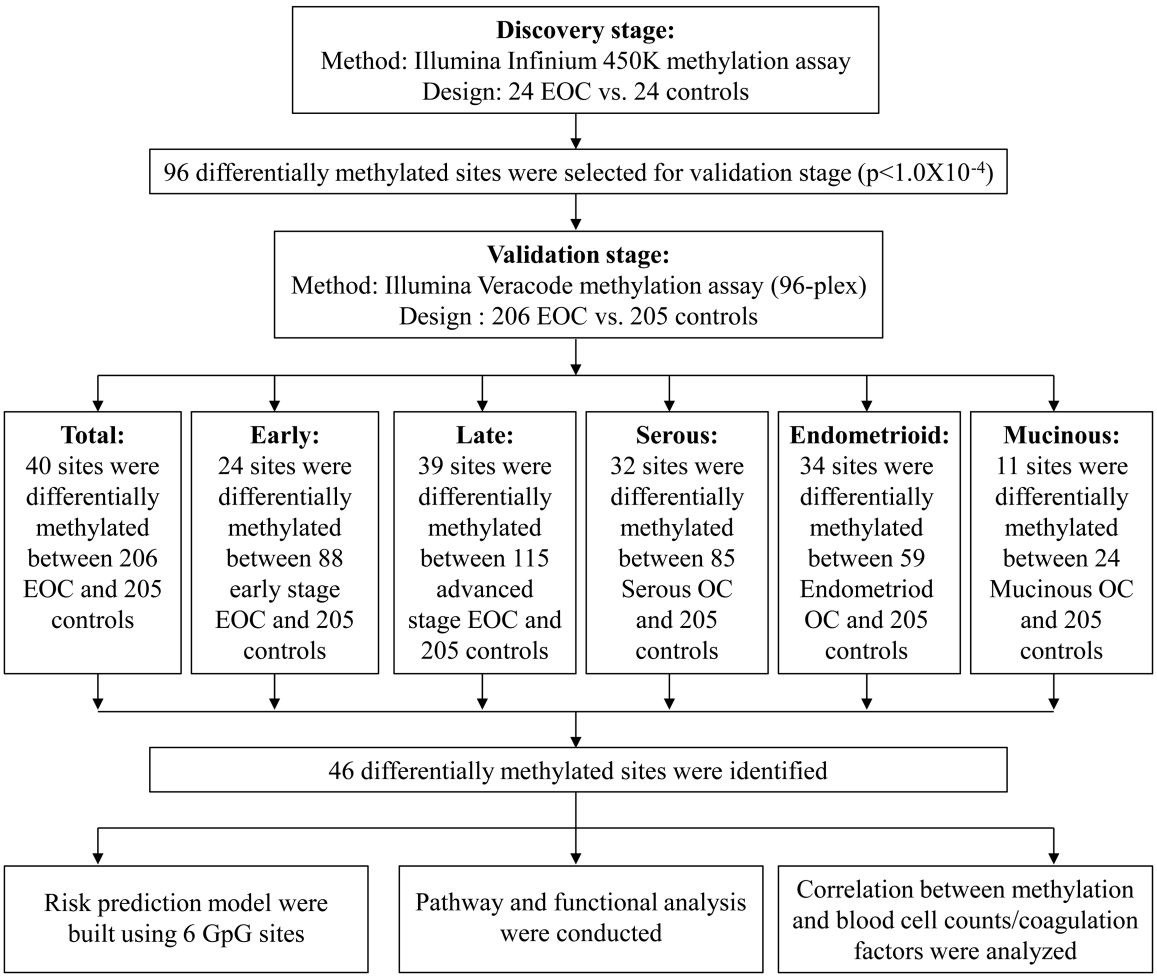

Figure 1. Schematic representation of the study design for methylation based biomarker discovery and validation.

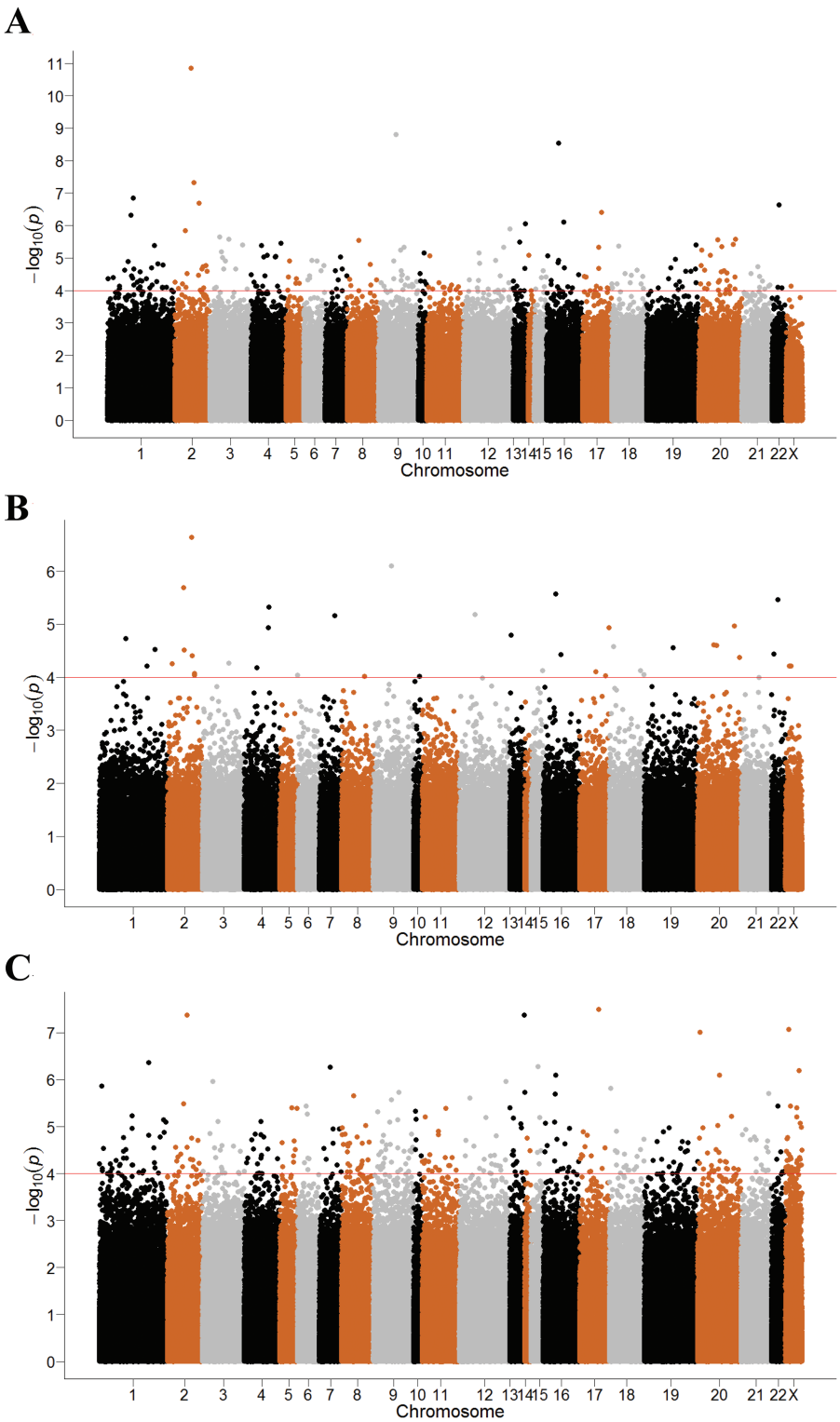

Figure 2. Epigenome-wide association results for EOC. Manhattan plot showing the epigenome-wide association results of all cases versus controls (**A**), early-stage cases versus controls (**B**), and advanced-stage cases versus controls (**C**). More than 485 000 CpG sites were analyzed. The x axis is the CpG site and y axis is negative logarithm of P-value ($-\log_{10}^{(P\ value)}$). The red horizontal line represents $P = 1.0 \times 10^{-4}$.

cg19716090, cg20956594, cg22534374 and cg22639787) were selected with prediction modeling to have an area under the ROC curve of 0.773 (0.729–0.818), suggesting that the six CpG sites predicted a higher risk for ovarian cancers than controls in 77.3% (Figure 4). The six CpG sties performed well when stratified by stage and histology subtype: Early stage AUC = 0.754 (0.693–0.816), Late stage AUC = 0.803 (0.754–0.853), Serous OC AUC = 0.773 (0.713–0.833), Endometrioid OC AUC = 0.799 (0.735–0.864) and Mucinous OC AUC = 0.725 (0.609–0.841) (Figure 4).

Illumina ID	Chr.	MapInfo	Nearest gene	Position in gene	Relation to CpG island	Total	Early stage	Advanced stage	Serous	Endometrioid	Mucinous
cg11937033	7	155150681	*BLACE*								
cg08450091	3	82857215	*CADM2*		*Island*						
cg22534374	1	201511610	*NAV1*		*S_Shelf*						
cg23327334	5	176855304	*GRK6*	*Body*	*S_Shore*						
cg25607383	6	30853569	*DDR1*	*5'UTR*	*S_Shore*						
cg12717729	1	24071253	*TCEB3*	*Body*	*S_Shore*						
cg01535567	16	698936	*WDR90*	*TSS1500*	*Island*						
cg22211672	15	74610366	*CCDC33*	*TSS1500*							
cg19716090	22	17560707	*IL17RA*		*N_Shelf*						
cg11453546	21	43990049	*SLC37A1*	*Body*	*Island*						
cg00066854	10	113987376	*TECTB*								
cg16962115	1	236016383	*LYST*	*TSS200*							
cg02756683	10	99449502	*MARVELD1*		*S_Shelf*						
cg02488385	21	36042752	*CLIC6*	*1stExon*	*Island*						
cg01286319	19	2695343	*GNG7*	*5'UTR*							
cg03002688	4	26152723	*RBPJ*								
cg01950479	22	23528162	*BCR*	*Body*	*S_Shelf*						
cg14559409	10	65930703	*CTNNA3*		*Island*						
cg14023999	15	90543224	*ZNF710*		*N_Shore*						
cg08365438	10	21683093	*CASC10*								
cg06415087	7	12726571	*ARL4A*	*TSS1500*	*Island*						
cg19138325	12	129429698	*GLT1D1*	*Body*	*Island*						
cg22441770	1	153929592	*CRTC2*	*Body*	*N_Shore*						
cg17833106	1	161060000	*GLRX2*	*TSS1500*							
cg16541275	17	78821754	*RPTOR*	*Body*	*S_Shelf*						
cg00207226	5	126407100	*C5orf63*	*5'UTR*	*N_Shore*						
cg16409562	14	21485900	*NDRG2*	*Body*							
cg12104982	19	5592815	*SAFB2*	*Body*	*N_Shore*						
cg26772894	16	85122558	*KIAA0513*	*3'UTR*							
cg27376514	17	17058422	*MPRIP*	*Body*	*N_Shelf*						
cg21933078	11	115024362	*CADM1*		*N_Shore*						
cg04515608	11	48129067	*PTPRJ*	*Body*							
cg06784563	18	77284509	*NFATC1*	*Body*	*Island*						
cg15125566	13	114876964	*RASA3*	*Body*	*Island*						
cg22639787	20	57464973	*GNAS*	*TSS1500*	*Island*						
cg09249800	1	6341287	*ACOT7*	*Body*	*Island*						
cg12049550	1	65035261	*CACHD1*	*Body*							
cg20956594	13	29202889	*POMP*								
cg20430870	10	52487619	*A1CF*								
cg24059119	19	30715575	*ZNF536*		*Island*						
cg17863551	19	43856594	*CD177*	*TSS1500*							
cg13888226	9	108282477	*FSD1L*	*Body*	*S_Shore*						
cg14380045	9	15527817	*C9orf92*		*Island*						
cg00414077	20	35504511	*SAMHD1*	*TSS200*							
cg09182724	1	193075640	*GLRX2*	*TSS1500*	*S_Shore*						
cg22972055	7	872293	*SUN1*	*5'UTR*							

FDR<1.0E-06
1.0E-06<FDR<1.0E-05
1.0E-05<FDR<1.0E-04
1.0E-04<FDR<1.0E-03
1.0E-03<FDR<5.0E-02
FDR>5.0E-02

Figure 3. Significantly differentially methylated sites in validation study. The heatmap represents the result of differential DNA methylation analysis of all cases versus controls (Total), early-stage cases versus controls (Early stage), advanced-stage cases versus controls (Advanced stage), serous ovarian cancer cases versus controls (Serous), endometrioid ovarian cancer cases versus controls (Endometrioid) and mucinous ovarian cancer cases versus controls (Mucinous). Differentially methylated sites ordered by FDR value of Total (all cases versus controls).

To identify the commonality of the 56 genes putatively regulated by the 46 different methylated CpG sites, we carried out pathway enrichment analysis utilizing the DAVID gene ontology (Figure 5). The top fold enrichment pathway was leukocyte mediated cytotoxicity and there were two genes included in the pathway were *LYST* (cg16962115, *FDR* = 1.24E–04) and *CADM1* (cg21933078, *FDR* = 1.22E–02). Most of the enriched pathways involved immune system process related pathways; we found that *NFATC1* (cg06784563, *FDR* = 1.46E–02) was included in immune system in Reactom pathway database (Supplementary Figure 9, available at *Carcinogenesis* Online). We found that the expression of *CADM1* (*P* = 2.87E–04) in blood cells was significantly lower in EOC patients than controls. But no significant expression differences were observed in *LYST* (*P* = 0.30) and *NFATC1* (*P* = 0.25) (Supplementary Figure 9, available at *Carcinogenesis* Online). In addition, we evaluated the correlation between differentially methylated CpG sites and blood cell counts/coagulation factors (Supplementary Table 5, available at *Carcinogenesis* Online). No significant correlation was observed between DNA methylation and blood cell counts except platelet count (Supplementary Figure 10, available at *Carcinogenesis* Online). We found that several CpG sites were correlated with platelet parameters and coagulation factors (Figure 6). Five platelet parameters (PLT: platelet count, PCT: plateletcrit, MPV: mean platelet volume, PDW: platelet distribution width and PLCR: platelet large cell ratio) and four coagulation factors (PT: prothrombin time, D-dimer, Fbg: plasma fibrinogen and AT III: Antithrombin III) were included in the correlation analysis. We found that four CpG sites (cg06784563, cg16541275, cg00207226 and cg00066854) were correlated with all the platelet parameters. For coagulation factors, there was no one correlated with all of the four coagulation factors. DNA methylation level of cg22441770 was correlated with both PT and AT III and there was 11 CpG sites were correlated with D-dimer.

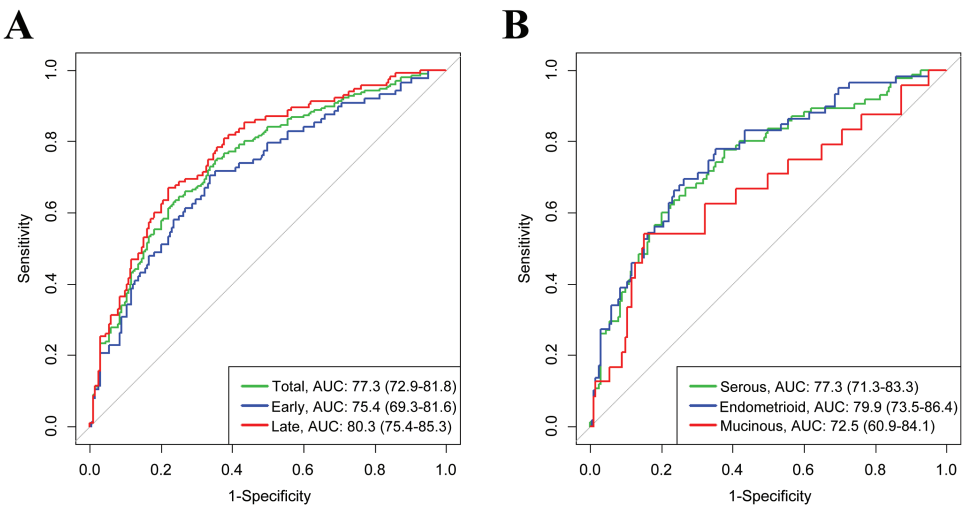

Figure 4. Receiver operating characteristics of six differentially methylated sites. (**A**) Area under the ROC curve for all cases versus controls (Total, green line), early stage cases versus controls (Early stage, blue line), and advanced stage cases versus controls (Advanced stage, red line) in predicting risk of ovarian cancer. (**B**) Area under the ROC curve for serous ovarian cancer cases versus controls (Serous, green line), endometrioid ovarian cancer cases versus controls (Endometrioid, blue line), and cases with mucinous pathology versus controls (Mucinous, red line) in predicting risk of ovarian cancer.

Discussion

In this two stage case–control epigenome-wide association study, we identified 46 novel CpG sites that were significantly associated with ovarian cancer in Han Chinese women. We also constructed a relatively high accuracy risk prediction model using six CpG sites, especially in early stage ovarian cancer. Pathway analysis using the genes with 46 significantly differentially methylated sites showed that they are parts of the immune system-related pathways. OC risk-associated differentially methylated CpG sites were not correlated with blood cell counts, but an association was observed with platelet parameters/coagulation factors. To our knowledge, this is the first report that revealed the correlation between DNA methylation in peripheral blood leukocyte and platelet parameters/coagulation factors.

Although the DNA methylation markers in peripheral blood have been reported in several types of cancers including breast, head and neck, ovarian, gastric, colorectal, and pancreatic cancer, the biological significance is uncertain (20). It is reported that DNA methylation was associated with lifestyle factors, dietary intake, and environmental exposure (21). Recently, increasing studies have been shown the relationship between DNA methylation with smoking and BMI (22,23). Previous studies speculated that the change of DNA methylation in peripheral blood may be due to the shift in blood cell components. To reveal the mechanism, Koestler *et al*. compared the DNA methylation between the subpopulations of leukocyte (including B cells, granulocytes, monocytes, NK cells, CD4+ T cells, CD8+ T cells and Pan-T cells) that were isolated from normal human peripheral blood leukocyte, they identified 50 CpG sites were significantly differentially methylated between the subpopulations of leukocytes (11). However, the 50 CpG sites were not statistically significant in our study, which is consistent with the previous report in breast cancer (9). In our study, DNA methylation sites related to ovarian cancer were not associated with leukocyte subpopulations. Interestingly, we found that DNA methylation in peripheral blood was correlated to platelet parameters and coagulation factors. Circulating blood platelets were reported to play a key role in the process of hemostasis, immunity, inflammation and cancer development/metastasis (8,24). In ovarian cancer, it is reported that platelet count was associated with EOC prognosis (25) and platelets could directly increase the proliferation of ovarian cancer cells (6). Global changes in DNA methylation during epithelial mesenchymal transition (EMT) in ovarian cancer could be induced by TGFβ1 (26) and the TGFβ1 secreted from platelet enhances an EMT in cancer cells (27). However, the mechanism of the relationship between platelet and DNA methylation in peripheral blood was still unknown, further studies are warranted.

In our study, we identified that genes with OC risk-associated differentially methylated CpG sites were involved the immune system process related pathways, including leukocyte mediated cytotoxicity, cell killing and immune effector process. Three genes, *NFATC1* (cg06784563), *LYST* (cg16962115) and *CADM1* (cg21933078) were enriched in the immune system process pathway. Cg06784563 was located at 5′ promoter flanking region of *NFATC1* that encodes nuclear factor of activated T-cells 1. NFAT proteins have been reported to have important functions in the immune system (28) and NFAT transcription factors have crucial role in many developmental programs including cancer (29). In ovarian cancer, *NFACT1* was significantly overexpressed in tumor tissues compared to paired normal control tissues and can promote proliferation up-regulating c-myc through activation of ERK1/2/p38/MAPK signal pathway in vitro (30). Cg21933078 was located at 15kb upstream of *CADM1* on chromosome 11, *CADM1* is a cell adhesion molecule and identified as a tumor suppressor in previous studies (31,32). The decreased expression of *CADM1* may conceivably be caused by promoter methylation thus promoting the tumor proliferation/invasion (31,32). In ovarian carcinoma, the downregulation of *CADM1* may serve as a biomarker of poor prognosis (33). *CADM1* have a novel function in suppression of metastasis by sensitizing tumor cells to immune surveillance mechanisms and *CADM1* loss is an important step in cancer immunoediting (34). Cg16962115 was located at 35 kb upstream of *LYST* that encodes lysosomal trafficking regulator at 1q42.3. Mutations in *LYST* were associated with Chediak–Higashi syndrome (35). There was no report about *LYST* on ovarian cancer or other cancers. Further studies are warranted to understand the implication of this gene in ovarian cancer.

Previous epigenome-wide association studies in ovarian cancer have identified differentially methylated CpG sites in

A

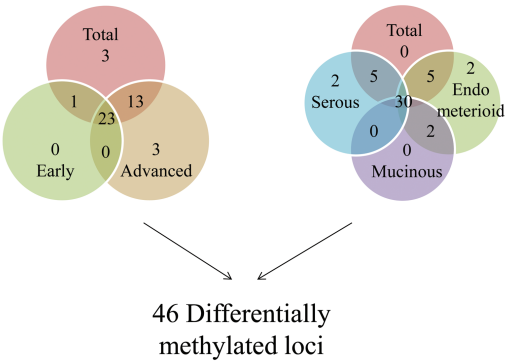

B

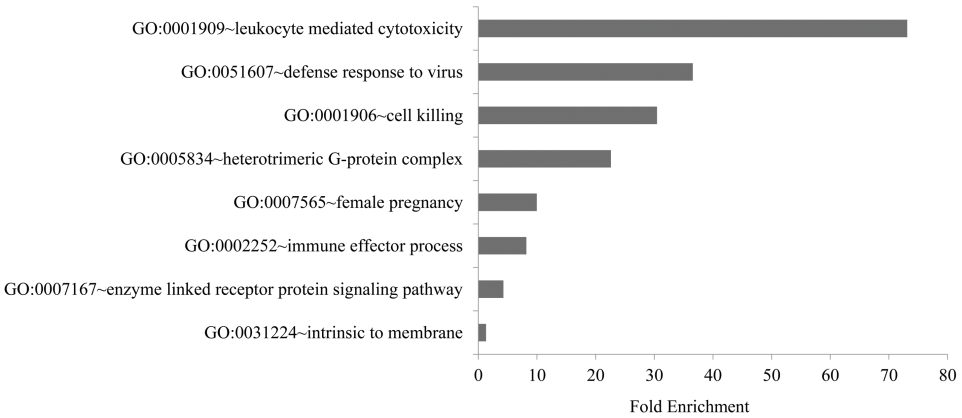

C

GO Term	Gene List
GO:0001909~leukocyte mediated cytotoxicity	CADM1, LYST
GO:0051607~defense response to virus	LYST, SAMHD1
GO:0001906~cell killing	CADM1, LYST
GO:0005834~heterotrimeric G-protein complex	GNG7, GNAS
GO:0007565~female pregnancy	GNAS, DDR1, FLT1
GO:0002252~immune effector process	CADM1, LYST, SAMHD1
GO:0007167~enzyme linked receptor protein signaling pathway	GNG7, DDR1, PTPRJ, FLT1
GO:0031224~intrinsic to membrane	CADM1, SEL1L3, SUN1, GRK6, GNAS, TECTB, IL17RA, RASA3, CACHD1, SLC37A1, GPAM, GNG7, PVRL4, MARVELD1, SGMS1, CD177, CLIC6, REEP3, CADM2, TCEB3

Figure 5. Gene ontology (GO) and pathway analysis of differentially methylated sites. (**A**) Venn diagram showed overlap of the significantly differentially methylated sites. (**B**) Significant GO terms (biological processes) associated with the 46 differentially methylated sites. The vertical axis represents the GO category, and the horizontal axis represents the fold enrichment of the significant GO terms. (**C**) Genes included in the pathway of GO term.

peripheral blood (12,16,17). However, none of them reached our selection criteria for validation ($P < 1.0 \times 10^{-4}$). These discrepant results were probably due to the following reasons: (1) the discovery stage of the previous studies was based on the Illumina's 27K Methylation Beadchip and the coverage of 450K that we used was much greater than previous studies. Of the 96 CpG sites that were selected for validation in our study, only one CpG site was included in the 27K methylation beadchip. (2) The populations of previous studies were European and our study population is Asian. It is well recognized that important differences exist between ethnic populations (36). In a recent GWAS study, we also found that the ovarian cancer risk loci discovered by GWAS in European population were not replicated in the Han Chinese population (37).

In summary, we have identified a set of blood-derived DNA methylation signatures that may be associated with EOC risk. Thus profiling of DNA methylation in peripheral blood may serve as novel tools for risk assessment and early detection in ovarian cancer. Validation study in large prospective cohorts and in-depth biological mechanistic research will be needed to validate these new biomarkers and develop strategies of epigenome therapy of ovarian cancer for precision medicine.

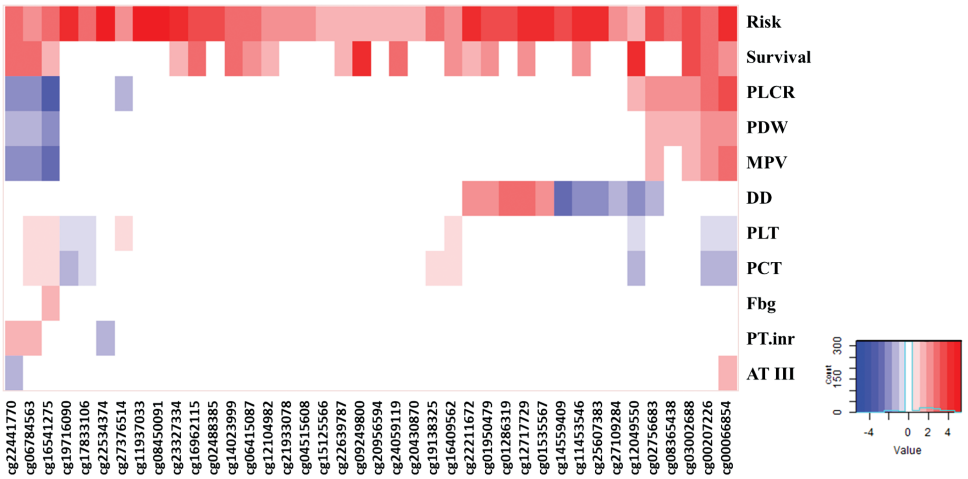

Figure 6. Correlation between DNA methylation and coagulation factors/platelet parameters. The degree of correlation and ovarian cancer risk/survival was represented based on $-\log_{10}$ (FDR) values in the heat map. For risk and survival, the color code in each heat map has been designated with white/light red as the lowest risk and dark red as the highest risk for ovarian cancer. For coagulation factors and platelet counts, a color code range from blue over white to red, red indicating positive correlation and blue indicating negative correlation. The increased positive correlation was shown in white to dark red, and negative correlation was shown in white to dark blue as indicated by the color scale. AT III, antithrombin III; DD, D-dimer; MPV, mean platelet volume; PLCR, platelet large cell ratio; PDW, platelet distribution width; PLT, platelet count; PCT, plateletcrit; Fbg, plasma fibrinogen; PT, prothrombin time.

Supplementary material

Supplementary data are available at *Carcinogenesis* online.

Funding

This work was supported by the National Natural Science Foundation of China (81320108022, 81502877, and 81470153), the Program for Changjiang Scholars and Innovative Research Team in University (PCSIRT) in China (IRT_14R40), Tianjin Science and Technology Committee Foundation (16JCYBJC26600), the American Cancer Society Research Professor Award.

Acknowledgements

The tissue bank is jointly supported by the Tianjin Cancer Institute and Hospital and the U.S. National Foundation for Cancer Research. WZ is supported by the Hanes and Willis Family Endowed Professorship in Cancer. We thank Mac B. Robinson at Wake Forest Baptist Comprehensive Cancer Center for editing this manuscript.

Conflict of Interest Statement: None declared.

References

1. Siegel, R.L. *et al.* (2016) Cancer statistics, 2016. CA. Cancer J. Clin., 66, 7–30.
2. Jayson, G.C. *et al.* (2014) Ovarian cancer. Lancet, 384, 1376–1388.
3. Miller, D.S. *et al.* (2009) Phase II evaluation of pemetrexed in the treatment of recurrent or persistent platinum-resistant ovarian or primary peritoneal carcinoma: a study of the Gynecologic Oncology Group. J. Clin. Oncol., 27, 2686–2691.
4. Salvi, S. *et al.* (2016) Cell-free DNA as a diagnostic marker for cancer: current insights. Onco. Targets. Ther., 9, 6549–6559.
5. Atkins, M.B. *et al.* (2016) Immunotherapy combined or sequenced with targeted therapy in the treatment of solid tumors: current perspectives. J. Natl. Cancer Inst., 108, djv414.
6. Cho, M.S. *et al.* (2012) Platelets increase the proliferation of ovarian cancer cells. Blood, 120, 4869–4872.
7. Davis, A.N. *et al.* (2014) Platelet effects on ovarian cancer. Semin. Oncol., 41, 378–384.
8. Franco, A.T. *et al.* (2015) Platelets at the interface of thrombosis, inflammation, and cancer. Blood, 126, 582–588.
9. Xu, Z. *et al.* (2013) Epigenome-wide association study of breast cancer using prospectively collected sister study samples. J. Natl. Cancer Inst., 105, 694–700.
10. Brennan, K. *et al.*; KConFab Investigators. (2012) Intragenic ATM methylation in peripheral blood DNA as a biomarker of breast cancer risk. Cancer Res., 72, 2304–2313.
11. Koestler, D.C. *et al.* (2012) Peripheral blood immune cell methylation profiles are associated with nonhematopoietic cancers. Cancer Epidemiol. Biomarkers Prev., 21, 1293–1302.
12. Koestler, D.C. *et al.* (2014) Integrative genomic analysis identifies epigenetic marks that mediate genetic risk for epithelial ovarian cancer. BMC Med. Genomics, 7, 8.
13. Dauksa, A. *et al.* (2014) DNA methylation at selected CpG sites in peripheral blood leukocytes is predictive of gastric cancer. Anticancer Res., 34, 5381–5388.
14. Pedersen, K.S. *et al.* (2011) Leukocyte DNA methylation signature differentiates pancreatic cancer patients from healthy controls. PLoS One, 6, e18223.
15. Wang, L. *et al.* (2010) Methylation markers for small cell lung cancer in peripheral blood leukocyte DNA. J. Thorac. Oncol., 5, 778–785.
16. Fridley, B.L. *et al.* (2014) Methylation of leukocyte DNA and ovarian cancer: relationships with disease status and outcome. BMC Med. Genomics, 7, 21.
17. Teschendorff, A.E. *et al.* (2009) An epigenetic signature in peripheral blood predicts active ovarian cancer. PLoS One, 4, e8274.
18. Winham, S.J. *et al.* (2014) Genome-wide investigation of regional blood-based DNA methylation adjusted for complete blood counts implicates BNC2 in ovarian cancer. Genet. Epidemiol., 38, 457–466.
19. Pils, D. *et al.* (2013) A combined blood based gene expression and plasma protein abundance signature for diagnosis of epithelial ovarian cancer–a study of the OVCAD consortium. BMC Cancer, 13, 178.
20. Li, L. *et al.* (2012) DNA methylation in peripheral blood: a potential biomarker for cancer molecular epidemiology. J. Epidemiol., 22, 384–394.
21. Noreen, F., *et al.* (2014) Modulation of age- and cancer-associated DNA methylation change in the healthy colon by aspirin and lifestyle. J. Natl. Cancer Inst., 106.
22. Breitling, Lutz P., *et al.* (2011) Tobacco-smoking-related differential DNA methylation: 27K discovery and replication. Am. J. Hum. Genet., 88, 450–457.
23. Dick, K.J. *et al.* (2014) DNA methylation and body-mass index: a genome-wide analysis. Lancet, 383, 1990–1998.
24. Leslie, M. (2010) Cell biology. Beyond clotting: the powers of platelets. Science, 328, 562–564.

25. Stone, R.L. *et al.* (2012) Paraneoplastic thrombocytosis in ovarian cancer. N. Engl. J. Med., 366, 610–618.
26. Cardenas, H. *et al.* (2014) TGF-β induces global changes in DNA methylation during the epithelial-to-mesenchymal transition in ovarian cancer cells. Epigenetics, 9, 1461–1472.
27. Labelle, M. *et al.* (2011) Direct signaling between platelets and cancer cells induces an epithelial-mesenchymal-like transition and promotes metastasis. Cancer Cell, 20, 576–590.
28. Müller, M.R. *et al.* (2010) NFAT, immunity and cancer: a transcription factor comes of age. Nat. Rev. Immunol., 10, 645–656.
29. Shou, J. *et al.* (2015) Nuclear factor of activated T cells in cancer development and treatment. Cancer Lett., 361, 174–184.
30. Xu, W. *et al.* (2016) NFATC1 promotes cell growth and tumorigenesis in ovarian cancer up-regulating c-Myc through ERK1/2/p38 MAPK signal pathway. Tumour Biol., 37, 4493–4500.
31. Woo, H.J. *et al.* (2015) Hypermethylation of the tumor-suppressor cell adhesion molecule 1 in human papillomavirus-transformed cervical carcinoma cells. Int. J. Oncol., 46, 2656–2662.
32. Wikman, H. *et al.* (2014) Loss of CADM1 expression is associated with poor prognosis and brain metastasis in breast cancer patients. Oncotarget, 5, 3076–3087.
33. Yang, G. *et al.* (2011) Loss/Down-regulation of tumor suppressor in lung cancer 1 expression is associated with tumor progression and is a biomarker of poor prognosis in ovarian carcinoma. Int. J. Gynecol. Cancer, 21, 486–493.
34. Faraji, F. *et al.* (2012) Cadm1 is a metastasis susceptibility gene that suppresses metastasis by modifying tumor interaction with the cell-mediated immunity. PLoS Genet., 8, e1002926.
35. Al-Tamemi, S. *et al.* (2014) Chediak-Higashi syndrome: novel mutation of the CHS1/LYST gene in 3 Omani patients. J. Pediatr. Hematol. Oncol., 36, e248–e250.
36. Henderson, B.E. *et al.* (2012) The influence of race and ethnicity on the biology of cancer. Nat. Rev. Cancer, 12, 648–653.
37. Chen, K. *et al.* (2014) Genome-wide association study identifies new susceptibility loci for epithelial ovarian cancer in Han Chinese women. Nat. Commun., 5, 4682.